



## Research Article

# Mathematical Modeling of Criteria Weighting and Risk Priority by Using Deviation Value Step-Wise in Energy Analysis for Double-Pipe Heat Exchangers

Farhad Gholami, Iraj Mirzaee, Mortaza Khalilian\*

Department of Mechanical Engineering, Faculty of Engineering, Urmia University, Urmia, Iran.

### PAPER INFO

#### Paper history:

Received: 07 July 2023

Revised: 04 December 2023

Accepted: 25 December 2023

#### Keywords:

Multi-Criteria Decision-Making,  
Mathematical Modelling,  
Failure Mode-Effects Analysis,  
Helical Double-Pipe Heat Exchanger,  
Energy Analysis

### ABSTRACT

Failure Mode and Effects Analysis (FMEA) is utilized for risk appraisal in various domains. In the FMEA methodology, each failure mode is evaluated by considering three risk factors: severity (S), occurrence (O), and detection (D). Subsequently, the Risk Priority Number (RPN) is obtained by multiplying these listed factors. This study introduces the Deviation Value Step-Wise Method (DVSM) as a new mathematical model for determining the scores of the SOD factors. This methodology consists of three main steps. Firstly, the FMEA technique is used to identify failure modes. Then, the DVSM is employed to assign weights to the SOD components. In this step, relative importance is determined based on linguistic variables. The third step involves ranking failure modes using the weighted RPN. Two general examples and a case study of two-pipe heat exchanger failure modes are considered to validate the proposed model and test the obtained results. The results demonstrate that the suggested approach has enhanced the overall prioritization of failure modes. This enables the Decision-Maker (DM) to identify primary failure modes and formulate corrective/preventive actions. Finally, both sensitivity analysis and energy efficiency investigation have been performed.

[https://doi.org/ 10.30501/jree.2024.399378.1596](https://doi.org/10.30501/jree.2024.399378.1596)

## 1. INTRODUCTION

### 1-1 Double-pipe heat exchangers

Heat exchangers are significant components utilized in various processes and research applications, including waste heat recovery processes, conversion systems, power production, cooling, etc. A two-tube heat exchanger is a type of heat exchanger used in different applications (Eduardo, 2010). Numerous researchers have focused on this type of heat exchanger. Maakoul et al. (2020) studied the thermo-fluid characteristics of a two-tube heat exchanger with split longitudinal fins on the annulus part. The thermodynamic analysis of the thermodynamic vent system heat exchanger was investigated by Liu et al. (2016). They established a semi-steady-state model to examine the thermal efficiency of a two-tube heat exchanger. Yildiz et al. (1996) conducted an experiment and analyzed the impact of propellers on heat transfer and pressure across a range of 2500 to 15000 for various propellers. Zarrella et al. (2013) performed a comprehensive comparison between helical tube and dual U-tube heat exchangers, examining thermal conductivity in both configurations. Maakoul et al. (2016) numerically studied the design and thermo-hydraulic efficiency of a two-tube heat exchanger with helical fins on the annulus side. Zanchini and Jahanbin (2017-2018) conducted an investigation on temperature distribution in borehole heat exchangers, offering a 3D simulation model for their numerical study. They also

analyzed a dual U-tube borehole heat exchanger using the finite element technique. Targui and Kahalerras (2008) conducted a numerical investigation of flow and heat transfer characteristics in a double-pipe heat exchanger with permeable constructions embedded in the sigmoid gap in two arrangements: (A) on the inner chamber, and (B) both chambers in a staggered fashion. Schmid et al. (2017) utilized ANSYS Fluent software package to study the air cooling system for street LED lights, proposing a type of dual tube heat exchanger for this system. Wenju et al. (2018) suggested a phase-change material (PCM)-based dual helicoidal heat exchanger for a heat pump, experimentally validating the heat storage. Qi et al. (2019) studied the thermal efficiency and pressure drop of titanium dioxide-water nanofluids in two-tube heat exchangers, discussing the impact of thermal fluid volume flow rates, nanoparticle mass fraction, nanofluid positions, nanofluid Reynolds numbers, and the designs of inner tubes on system efficiency.

### 1-2 MCDM and FMEA

In multi-standard investigation methodologies, a critical challenge arises in determining the weights and loads of criteria values. The subsequent crucial step in multi-criteria decision-making (MCDM) involves selecting a suitable strategy for establishing model weights, which complicates the dynamic cycle. Recognizing how the weight values of each criterion significantly impact the decision-making process, specific attention should be devoted to the objectivity variables of

\*Corresponding Author's Email: [m.khalilian@urmia.ac.ir](mailto:m.khalilian@urmia.ac.ir) (M. Khalilian)

URL: [https://www.jree.ir/article\\_186787.html](https://www.jree.ir/article_186787.html)

Please cite this article as: Gholami, F., Mirzaee, I. & Khalilian, M. (2024). Mathematical Modeling of Criteria Weighting and Risk Priority by Using Deviation Value Step-Wise in Energy Analysis for Double-Pipe Heat Exchangers, *Journal of Renewable Energy and Environment (JREE)*, 11(1), 122-134. <https://doi.org/10.30501/jree.2024.399378.1596>.



criteria loads. Over the past few years, investigators have introduced various strategies. One such method is the Analytical Hierarchy Process (AHP).

For instance, [Benmoussa et al. \(2019\)](#) proposed an ergonomic assessment criteria approach, employing the AHP multi-criteria prioritization strategy to select and prioritize measures. Similarly, [Miciuła and Grunt \(2019\)](#) advocated for the AHP choice technique in the context of power providers. In a comprehensive approach combining Weight-of-Evidence (WOE) and AHP, [Chen et al. \(2021\)](#) conducted an examination of housing adaptability criteria to predict the Suitable Growth Area (SGA) under different ecological scenarios. This study involved 412 WH events and 15 environmental factors in Guangdong, South China, considering meteorological and hydro-sensible attributes across various seasons.

Moreover, [Sedghiyan et al. \(2021\)](#) focused on gathering not-depleted-by-use resources in five environmental districts in Iran, utilizing AHP, TOPSIS, and SAW techniques. It is noteworthy that the inclusion of diverse methodologies in these studies underscores the importance of a nuanced approach in addressing the complex challenges of multi-criteria decision-making methodologies.

The Best Worst Method (BWM), introduced in 2015, is a noteworthy multi-criteria decision-making approach. [Torkayesh et al. \(2021\)](#) applied this method to develop an integrated decision-making technique for determining landfill areas in medical care waste systems. Their study utilized a combination of Geographic Information System (GIS), Best Worst Method, and a trade-off arrangement strategy based on the grey domain set, considering sustainability agents. Moving on, [Balali et al. \(2021\)](#) evaluated the risks associated with urban natural gas systems in Shiraz. Their study employed negotiation, opinion polls, and contextual data analysis as research tools. COPRAS (Complex Proportional Assessment) was used for risk assessment, and the ANP (Analytic Network Process) procedure aided in assigning weights to each risk evaluation measure.

[Luo et al. \(2020\)](#) proposed a novel technique for selecting the optimal site for a Waste-To-Energy (WTE) incineration plant. Additionally, [Yücenur and Ipekçi \(2020\)](#) addressed the location issue for the first marine current energy production plant in Turkey. In their paper, an MCDM (Multi-Criteria Decision-Making) approach was introduced, incorporating four main indicators, 12 indexes, and three alternatives. The SWARA strategy determined the weights of criteria, and the alternatives were ranked using the WASPAS technique.

Furthermore, [Balki et al. \(2020\)](#) conducted a study confirming that the optimal operating parameters of an SI engine filled with pure C<sub>2</sub>H<sub>6</sub> and CH<sub>4</sub> as substitute fuels were determined through MCDM using experimental data. This analysis considered efficiency, emission, and ignition parameters in the decision-making process. The integration of these methods showcases the versatility and applicability of multi-criteria decision-making in various domains, emphasizing its role in addressing complex issues and optimizing decision outcomes.

Focusing on the issue that the multi-objective assessment of proficiency and the weighting modulus of records was hard to track down, a fluffy extensive execution assessment strategy for rolling linear guide (RLG) was proposed by [Ma et al. \(2020\)](#). Attending to the static and dynamic lists, in their investigation, a design model containing nine weighting moduli was developed. [Wang et al. \(2020\)](#) developed a successive three-way decision-making methodology dependent on BWM

(best-worst technique) and MULTIMOORA for numerous degrees of granularity to manage the multi-characteristic collective choice-making issues under uncertainty. [Bahrami et al. \(2019\)](#) traced the prosperous utilization of a novel half-breed MCDM called BWM-ARAS for coordinating a multi-source geographical informational index to outline exceptionally Cu imminent areas in the Abhar territory, Northwest of Iran. [Lahri et al. \(2021\)](#) proposed a two-stage multi-target feasibility number linear programming practical supply chain design model, minimizing financial and environmental goals and maximizing social sustainability objectives. The offered model determined the capacities of facilities and the amount of the flow of goods across the supply chain. The fuzzy best-worst method was used by [Khazaeili et al. \(2019\)](#) to weigh supplier selection criteria. Later, they used the piecewise linear values function to rank suppliers. The proposed strategy addressed the issue of sustainable supplier selection in the oilseed professions as a case study in the food supply chain. [Ghoushchi and Khazaeili \(2019\)](#) introduced a novel concept idea named G-numbers to reduce data uncertainty based on importance and necessity concepts. In G-numbers, G= (I, N), I was the important component, and N was the necessary part of the real-valued uncertain variables. In general, I and N were described as linguistic variables. This team, in other works ([2019,2021](#)), employed importance, necessity, and reliability concepts to demonstrate these parameters' applications and effects in MCDM issues. [Sari \(2021\)](#) proposed a study on woodland fire susceptibility where the weight of every criterion is determined by employing the AHP method. Later, TOPSIS and VIKOR strategies were utilized to generate woodland fire susceptibility maps in the Muğla area. [Chodha et al. \(2021\)](#) used the MCDM approach dependent on the TOPSIS strategy to choose an industrial robot for the arc welding operation. Using the TOPSIS method to perform a comprehensive environmental impact assessment for concrete mixing station (CMS) performed by [Lin et al. \(2021\)](#). They used this method to determine the optimal location of CMS. Parameters like elasticity, hardness, softening point, density, and cost were chosen and optimized by [Avikal et al. \(2021\)](#) using MCDM. Using Fuzzy AHP and TOPSIS, all criteria were compared among them pairwise to create a rational matrix.

As previously mentioned, FMEA is a subjective tool used to identify and evaluate the effects of a specific flaw or failure mode at a component ([Long, 2014](#)). There are various investigations into this issue. [Xin et al. \(2021\)](#) proposed a prevailing failure modes analysis technique based on the differential evolution algorithm, which generated sample points on the limit state plane and used the differential evolution algorithm to optimize. [Okabe and Otsuka \(2021\)](#) developed a validation method for the rational relationship between the design deviations, possible damage/fracture modes, and the eventual failure modes using SVM. They stated that the Regular Failure Modes and Effects Analyses lack a specific process to ensure potential damage/fracture of component materials. [Hoisak et al. \(2021\)](#) aimed to benchmark the effectiveness of FMEAs for electronic brachytherapy of the skin and the breast by comparing the predicted versus actual failure modes reported in different incident learning systems. [Chin et al. \(2008\)](#) reported in their study that every failure mode can be assessed by three components: severity, the probability of occurrence, and the failure mode detection. They demonstrated that in a typical FMEA assessment, a number from 1 to 10 (with 1 being the best and 10 being the worst-case scenario) was assigned for each of the three elements. By

multiplying the values for S, O, and D, a risk priority number was obtained, which was  $RPN = S \times O \times D$ . [Hu et al. \(2021\)](#) assessed the hazard and risk (HR) resulting from the induced seismic through the Entropy-Fuzzy-AHP (E-FAHP) method. An approach in several steps to address some of the shortcomings of the FMEA method was proposed by [Khazaeili et al. \(2019\)](#). Firstly, the detection of the FMs and assigning of the Risk Priority Number (RPN) values representatives were performed using the FMEA. The next step involved the Fuzzy Best-Worst Method to quantify the weights of these variables. Finally, the outputs of the previous steps were used as a basis to prioritize the failures using the proposed MOO by Ratio Analysis based on the Z-number theory (Z-MOORA). [Dorosti et al. \(2020\)](#) conducted a study on the management of people's waiting time in a clinic using fuzzy-based failure mode and impact analysis. Eleven risk factors resulted in the prolongation of waiting time introduced by practitioners to address the typical FMEA deficiency. [Khalilzadeh et al. \(2021\)](#) identified and assessed the principal risks of oil and gas projects under uncertain conditions. The main risks were identified through document analysis, which was reduced to 17 risks through expert opinions using the fuzzy Delphi method. [Subriadi and Najwa \(2020\)](#) examined the consistency of both conventional FMEA and improved FMEA in IT risk assessment. The relationship between RPN factors in the fuzzy process FMs and impact analysis and overall equipment effectiveness in the production cycle is described by [Baghbani et al. \(2019\)](#). [Ouyang et al. \(2021\)](#) introduced a data integration FMEA strategy based on dual tuple linguistic data and interval probability. The dual tuple linguistic set theory was adopted to transform the heterogeneous data into interval numbers. Furthermore, the interval probability analysis method was applied to analyze failure modes.

As mentioned before, heat exchangers are one of the most widely used equipments in various industries. The principled and correct design of these types of equipment has always been the desire of design engineers because, in numerical simulations, assumptions are always made to simplify the problem, which causes differences in numerical results and experimental data. Therefore, providing a method to involve real and existing phenomena in the design can open the way for design engineers.

This paper uses a novel methodology named DVSM to weigh the SOD factors to prioritize the failure modes. The proposed approach includes a weighted RPN instead of a traditional one. The organization of this work is as follows. Section 2 contains a detailed definition of the DVSM strategy with two illustrating examples. Section 3 is dedicated to proposing a new approach utilizing the FMEA procedure, DVSM, and weighted RPN techniques to assess the failure modes and rank them. In Section 4, a case study of the two-tube heat exchanger is presented and analyzed. Ultimately, the final section includes sensitivity and energy analysis.

## 2. Deviation Value Step-wise Method (DVSM)

Genuine issues lack an inherent indicator of equal importance. Therefore, it is crucial to precisely define the essential elements of specific indicators by employing appropriate weight coefficients. Selecting weights for various criteria in Multiple Criteria Decision-Making (MCDM) methodologies consistently poses a challenge intertwined with subjectivity. This process is pivotal and significantly influences

the outcome, as weight coefficients play a critical role in the determination of the arrangement.

Hence, meticulous attention is required to decide on the weights, and the Decision Vector Space Model (DVSM) is presented as a model for detecting these weight coefficients. This strategy facilitates the precise determination of the advantages of the weight coefficients for all elements considered at a specific level of the hierarchy while ensuring the conditions of analytical consistency are met. The DVSM method plays a crucial role in accurately determining the weights of the indicators. The steps involved in DVSM, utilized for this purpose, have been succinctly outlined in this passage.

### Step 1. Criteria Detection by the Decision-maker (DM)

Suppose a decision-maker identifies  $n$  criteria  $\{C_1, C_2, \dots, C_n\}$  for making a decision. The DM ranks among the criteria regarding their importance degree, from the highest importance to the least significant, as follows:

$$C_n > C_{n-1} > \dots > C_2 > C_1 \tag{1}$$

### Step 2. Sequential comparisons between criteria

In this step, the sequential comparisons between  $c_j$  and  $c_{j+1}$  in the step-wise process are determined, as shown in Table 1. The relative importance of the  $j^{th}$  criteria to the  $(j + 1)^{th}$  one using Table 1 is achieved, and its set is introduced as follows (Figure 1):

$$a_{j,j+1} = \{a_{12}, a_{23}, \dots, a_{n-1,n}\} \tag{2}$$

**Table 1.** Linguistics variable for criteria

Linguistic terms	Score
Equal importance (EI)	1
Extremely Low importance (ELI)	1.1
Very Low importance (VLI)	1.2
Low importance (LI)	1.3
Lower Moderate importance (LMI)	1.4
Moderate importance (MI)	1.5
Upper Moderate importance (UMI)	1.6
High importance (HI)	1.7
Very High importance (VHI)	1.8
Extremely High Importance (EHI)	1.9

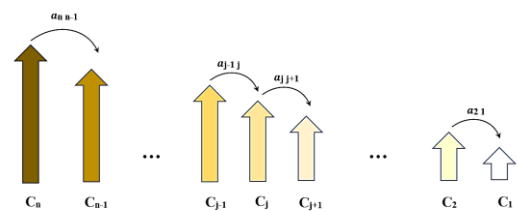


**Figure 1.** Pairs comparisons among criteria

### Step 3. The optimal weights $(w_1^*, w_2^*, \dots, w_n^*)$

To find the optimal weight for each pair  $w_j/w_{j+1} = a_{j,j+1}$ , the relative deviation of the sum of the least squares

$\sqrt{\sum_{j=1}^{n-1} (w_j/w_{j+1} - a_{j,j+1})^2}$  should be minimized. Therefore, the following mathematical model is presented:

$$\text{Min } z = \sqrt{\sum_{j=1}^{n-1} (w_j/w_{j+1} - a_{j,j+1})^2} \tag{3}$$

$$\text{s.to: } \sum_{j=1}^n w_j = 1 \tag{4}$$

$$w_j \geq 0 \tag{5}$$

The linearized form of the mathematical model is given as follows:

$$\text{Min } z = \sqrt{\sum_{j=1}^{j=n-1} (w_j - a_{jj+1}w_{j+1})^2} \tag{6}$$

$$\text{s.to: } \sum_{j=1}^{j=n} w_j = 1 \tag{7}$$

$$w_j \geq 0 \tag{8}$$

Proof. It must be proved that Equations (3)-(5) are equivalent to (6)-(8).

In objective function (3), the relative deviation term should be as follows:

$$w_j/w_{j+1} = a_{jj+1} \tag{9}$$

The simplified form of Equation (9) will be:

$$w_j - a_{jj+1}w_{j+1} = 0 \tag{10}$$

Solving the problems (6)-(8), the optimal weights  $w_j^*$  for  $j = 1, 2, \dots, n$  and optimal value  $z^*$  are obtained.

The DVSM has some notable benefits that make it a dependable and intriguing model. The advantages of DVSM are demonstrated by contrasting it with the various techniques for determining the weight coefficients of criteria. To perform an acceptable comparison, the BWM, AHP, and FUCOM strategies were placed in the center since the validity of these methods relies on gathering the states of numerical transmissibility and the pairwise comparison of the criteria. [۳۶]

The AHP, BWM, and FUCOM have  $n(n-1)/2$ ,  $(2n-3)$ , and  $(n-1)$  numbers of pairwise comparisons of the  $n$  number criteria, respectively (Table 2). Thus, the FUCOM has less pairwise comparisons. Both BWM and FUCOM use mathematical and numerical techniques to achieve the criterion weight. The number of constraints for both techniques is  $2(n-1)$ . On the other hand, the proposed DVSM has  $(n-1)$  pairwise comparison and is just one limitation of the mathematical model. Therefore, the DVSM experiences a shorter amount of calculation time than other techniques.

**Table 2:** The required number of comparisons based on the number of constraint functions

MCDM tech.	The quantity value of criteria (n) and the necessary number of pairwise comparisons															
	n = 2		n = 3		n = 4		n = 5		n = 6		n = 7		n = 8		n = 9	
	PC*	NCF*	PC	NCF	PC	NCF	PC	NCF	PC	NCF	PC	NCF	PC	NCF	PC	NCF
AHP $n(n-1)/2$	1	--	3	--	6	--	10	--	15	--	21	--	28	--	36	--
BWM $(2n-3)$	1	2	3	4	5	6	7	8	9	10	11	12	13	14	15	16
FUCOM $(n-1)$	1	2	2	4	3	6	4	8	5	10	6	12	7	14	8	16
DVSM $(n-1)$	1	1	2	1	3	1	4	1	5	1	6	1	7	1	8	1
*PC: Pair Comparison			*NCF: Number of Constraint Function													

To validate the proposed model and test the obtained results, two general examples and one case study on a double-pipe heat exchanger are displayed.

**Example 1.**

This basic model includes choosing a heat exchanger configuration for an organization to provide the required heat flux to represent the DVSM steps above. The organization recognizes three choice models as  $C_1$ : load adaptability,  $C_2$ : accessibility,  $C_3$ : cost (Rezaei, 2015).

Solution:

At first, the ranks of the criteria are deduced by DM considering the importance as follows:

$$C_3 > C_2 > C_1$$

Based on Table 1, the relative importance of  $C_3$  to  $C_2$  is Lower Moderate importance (LMI) while  $C_2$  to  $C_1$  is of High importance (HI). Therefore  $a_{32} = 1.4$  and  $a_{21} = 1.7$ . Therefore, the results in Equations (3)-(5) for this example are:

$$\text{Min } z = \sqrt{(w_3 - 1.4w_2)^2 + (w_2 - 1.7w_1)^2}$$

$$\text{s.t.o: } w_1 + w_2 + w_3 = 1$$

$$w_1, w_2, w_3 \geq 0$$

Upon solving this model, we find  $w_1^* = 0.197$ ,  $w_2^* = 0.335$ ,  $w_3^* = 0.468$  and  $z^* = 0$ .

**Example 2.**

When purchasing a vehicle, a purchaser considers five indicators, including quality ( $C_1$ ), cost ( $C_2$ ), solace ( $C_3$ ), safety ( $C_4$ ), and style ( $C_5$ ). The purchaser gives the accompanying pairwise examination vectors (Rezaei, 2015).

Solution:

At first, the ranks of the criteria are deduced by DM considering the importance as follows:

$$C_2 > C_1 > C_4 > C_3 > C_5$$

Based on Table 1, the relative importance of  $C_2$  to  $C_1$  is High importance (HI),  $C_1$  to  $C_4$  is Very Low importance (VLI),  $C_4$  to  $C_3$  is Extremely Low importance (ELI), and  $C_3$  to  $C_5$  is Moderate importance (MI). Therefore  $a_{21} = 1.7$ ,  $a_{14} = 1.2$ ,  $a_{43} = 1.1$ , and  $a_{35} = 1.5$ . Thus, the results in Equations (3)-(5) for this example are:

$$\text{Min } z =$$

$$\sqrt{(w_2 - 1.7w_1)^2 + (w_1 - 1.2w_4)^2 + (w_4 - 1.1w_3)^2 + (w_3 - 1.5w_5)^2}$$

$$\text{s.t.o: } w_1 + w_2 + w_3 + w_4 + w_5 = 1$$

$$w_1, w_2, w_3, w_4, w_5 \geq 0$$

By solving this model, we find  $w_1^* = 0.209$ ,  $w_2^* = 0.354$ ,  $w_3^* = 0.158$ ,  $w_4^* = 0.174$ ,  $w_5^* = 0.105$  and  $z^* = 0$ .

**3. Offered approach**

In this segment, the suggested approach of this investigation utilizing the FMEA procedure, DVSM, and weighted RPN



techniques is introduced to evaluate the failure modes and rank them. Three RPN variable values are given in Table 3 .

- In the initial step of this methodology, FMs are distinguished by the Decision Maker (DM) group inside the risk evaluation domain. The values of the SOD factors are decided. In the customary FMEA for estimation of RPN score, the SOD factors are rated customarily from 1 for the most reduced degree to 10 for the most elevated .
- In the subsequent stage, DVSM is utilized to propose various loads of the SOD agents. In this stage, the DVSM stages are carried out to decide the heaviness of each hazard factor .
- In the next stage, the yields of previous stages have been utilized as a premise to focus on the distinguished failure modes utilizing the Weighted Risk Priority Number (W-RPN) technique. The final rank of FMs is used to analyze sensitivity and energy efficiency. Figure 2 shows the proposed approach flowchart.

**Table 3:** Conventional appraisals for RPN factors (Baležentis et al. 2012)

Rating	S	O	D
10	Hazardous without warning	Very high: Almost failure is inevitable	Absolute uncertainty
9	Hazardous with warning		
8	Very high	High: repeated failures	High: repeated failures
7	High		
6	Moderate	Moderate: occasional failures	Moderate: occasional failures
5	Low		
4	Very low		
3	Minor	Low: relatively few failures	Low: relatively few failures
2	Very minor		
1	None	Remote: unlikely failures	Remote: failure is unlikely

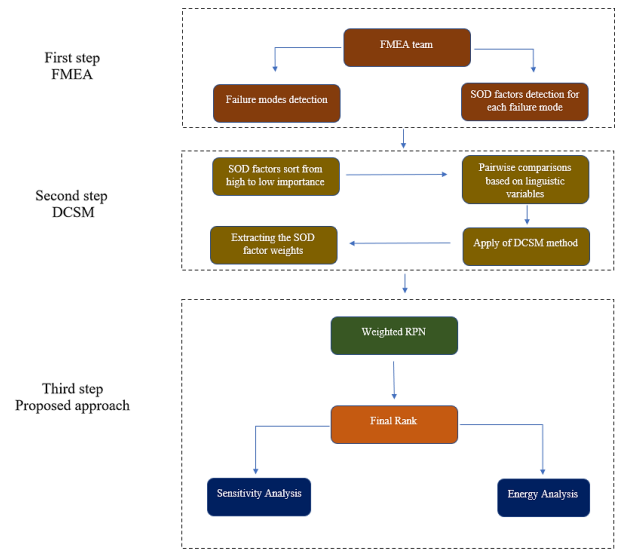


**Figure 2.** Proposed approach flowchart

**4. CASE STUDY**

Heat exchange constitutes a fundamental aspect within a thermal framework, necessitating the refinement of device arrangements (Almerbati, 2021). Heat exchangers serve the crucial role of transferring heat energy between two fluids with disparate temperatures. These versatile devices find application in various domains, including chemical processing, mechanical radiators, solar-powered systems, vehicles, and power plants (Abu-Hamdeh et al. 2020). Notably, there exist different types of heat exchangers, and the helical-pipe configuration stands out among them.

The helical-pipe design introduces a radial component of force owing to the curvature of the pipe. This feature fosters an auxiliary flow pattern perpendicular to the primary axial flow, facilitating both fluid mixing and enhanced heat transfer. Consequently, the use of helical tubes in the heat exchange process proves to be highly efficient when compared to straight pipes (Mehrabi et al. 2013).

Numerous investigations have delved into this subject, with a range of studies conducted (Li, 2021- Maddah, 2018- Kumar, 2018- Pashae, 2012- Pashae, 2018- Pashae, 2021). In a numerical exploration, Pashae et al. (2011) scrutinized vital parameters in a two-tube heat exchanger. Figure 3 illustrates the configuration of their primary model, showcasing the positions of considered failure modes in this specific type of heat exchanger. The insights gained from these studies contribute significantly to our understanding of heat exchange processes and underscore the importance of innovative design in optimizing thermal systems.

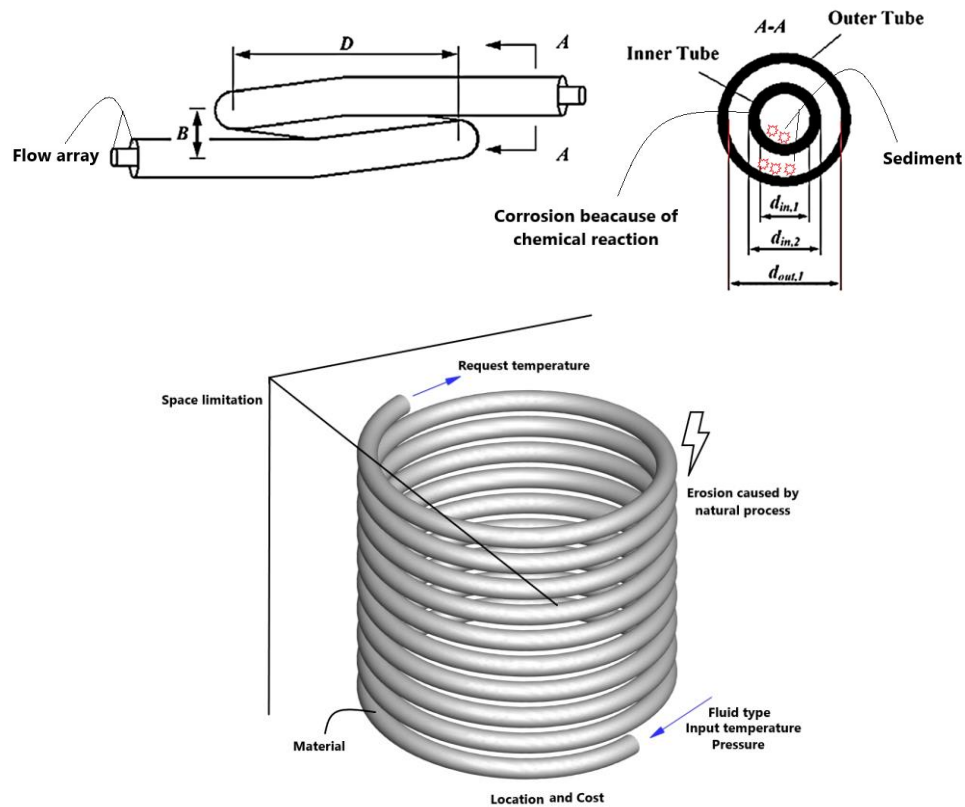


Figure 3: Failure modes position in a helicoidal double-tube heat exchanger [Pashae et al. \(2011\)](#)

Although the heat exchangers are generally intended for an ordinary life of over ten years, their real service life, notwithstanding, shifts from 2-3 to 6-8 years, contingent upon the service conditions and obviously on the nature of warmth move media. The sort of scale contrasts from one industry to another, contingent upon the mineral substance of the accessible fluid [\(Vasauskas et al., 2006\)](#).

**Assumptions :**

As previously mentioned, the helical type of heat exchanger boasts significant advantages, but its performance is subject to several critical parameters referred to as failure modes. These factors can detrimentally impact the heat exchanger's efficiency. According to Table 4, Operation limit, Sediment, Corrosion, Erosion, Fluid type, Input temperature, Request temperature, Pressure, Material, Flow array, Location, and Cost constitute a category of failure modes

considered in the present work [\(Vasauskas et al., 2006\)](#). The primary objective of the current study is to identify the key factors that should be taken into account in heat exchanger design.

Initially, it is assumed that Failure Modes (FMs) are specified by the Decision Maker (DM). The values of the SOD factors are determined (refer to Table 4). Subsequently, the Decision Variable Selection Method (DVSM) is employed to propose various loads for the SOD agents. At this stage, DVSM stages are executed to determine the significance of each hazard factor. Ultimately, the results obtained from the preceding steps serve as a basis to focus on the distinguished failure modes using the Weighted Risk Priority Number (W-RPN) technique. The final ranking of FMs is then utilized to assess energy efficiency.

Table 4: Double-pipe heat exchanger failure modes [\(Pashae et al., 2011- Vasauskas et al., 2006\)](#)

Failure modes	Definitions	S	O	D
Fm <sub>1</sub>	Operation limit: lack of space for heat exchanger installation	9	8	3
Fm <sub>2</sub>	Sediment: matter that settles to the bottom	9	9	2
Fm <sub>3</sub>	Corrosion: the process of corroding metal	7	7	4
Fm <sub>4</sub>	Erosion: being eroded procedure caused by air, water, and so on	7	6	5
Fm <sub>5</sub>	Fluid type: working fluid physical features	5	5	4
Fm <sub>6</sub>	Input temperature: entrance temperature for fluid	6	8	5
Fm <sub>7</sub>	Request temperature: purpose temperature for outflow fluid	4	9	6
Fm <sub>8</sub>	Pressure: the pressure that the device works in	5	6	8
Fm <sub>9</sub>	Material: the matter from which the device is made	4	4	7
Fm <sub>10</sub>	Flow array: if the various arrays of flow (parallel and counter) affect the heat exchanger proficiency	6	6	5
Fm <sub>11</sub>	Location: the place that the device is installed in	4	3	8
Fm <sub>12</sub>	Cost: an amount that has to be paid to produce the device	7	7	5

## 5. Analysis of the results

The outcomes acquired from the offered approach for prioritization of the two-tube heat exchanger failures are introduced in this segment. As indicated by the principal period of this methodology (Figure 2), the FMs are first distinguished by the FMEA team, and then, for each FM, the values of SOD factors are determined based on linguistic variables (Table 3). These SOD factor values for the 12 FMs are represented in Table 4 regarding the FMEA team concept. Next, DVSM has been applied to determine the SOD factors' weight using Table 1. Finally, the third step will be as follows: Solution:

At first, the criteria are ranked by DM based on the importance as follows:

$$S > O > D$$

Based on Table 1, the relative importance of  $S$  to  $O$  is Very Low importance (VLI) and  $O$  to  $D$  is Moderate importance (MI). Therefore,  $a_{SO} = 1.2$  and  $a_{OD} = 1.5$ . Therefore, the results in Equations (3)-(5) for this example are:

$$\text{Min } z = \sqrt{(w_S - 1.2w_O)^2 + (w_O - 1.5w_D)^2}$$

s.t.o:  $w_S + w_O + w_D = 1$

$$w_S, w_O, w_D \geq 0$$

Upon solving this model,  $w_S^* = 0.419$ ,  $w_O^* = 0.349$ ,  $w_D^* = 0.232$ , and  $z^* = 0$ .

To rank the failure modes by weighted RPN method, it is represented as:

$$\text{Weighted RPN}_i = (a_{iS}w_S) \times (a_{iO}w_O) \times (a_{iD}w_D); \quad i = 1, 2, \dots, n \quad (11)$$

$w_S$ ,  $w_O$ , and  $w_D$  are the weights of SOD factors, respectively.  $a_{iS}$ ,  $a_{iO}$ , and  $a_{iD}$  are the components of the  $i^{\text{th}}$  failure concerning SOD factors.  $\text{Weighted RPN}_i$  is the value of the  $i^{\text{th}}$  failure mode.

Table 5 presents the outcomes of the Traditional Risk Priority Number (RPN) analysis. In this analysis, failure mode Fm12 with an RPN of 245 holds the top rank. The second rank is shared by failure modes Fm6 and Fm8, both having an RPN of 240. Meanwhile, failure modes Fm1 and Fm7, with an RPN of 216, are placed in the third rank. This categorization results in ten classes during the failure prioritization process.

However, an examination of failure prioritization based on the traditional RPN reveals a lack of comprehensive prioritization for the Failure Modes (FMs). Consequently, this can create confusion for Decision Makers (DM) involved in risk management. Notably, Table 5 suggests that the incomplete prioritization might be attributed to neglecting the weight of Specific Operational Design (SOD) factors.

A comparison between the outcomes of the weighted RPN and the traditional RPN indicates that the failure modes, previously sharing the same rank in the traditional analysis, are now divided into twelve classes. Further scrutiny reveals that failure modes Fm6 and Fm8, initially placed in the 2nd rank based on the traditional RPN, now find themselves in the fourth and eighth ranks, respectively, according to the proposed technique. Interestingly, Fm2, which held the 7th rank in the traditional RPN, now claims the first position. This shift underscores the effectiveness of the Design Variable Sensitivity Matrix (DVSM) weighting strategy in appropriately highlighting high-risk criteria.

For a more detailed visual representation, Figure 4 illustrates a side-by-side comparison of the traditional and weighted RPN results. The contrast between these approaches underscores the significance of incorporating weighted factors for a more nuanced understanding of risk prioritization in Failure Mode and Effects Analysis (FMEA).

**Table 5:** Prioritization of the FMs dependent on the weighted RPN

Failure mode		Risk Factors			Conventional FMEA		Proposed FMEA	
		S	O	D	Traditional RPN	Initial Rank	Weighted RPN	Final Rank
Fm <sub>1</sub>	Operation limit	9	8	3	216	3	7.256	2
Fm <sub>2</sub>	Sediment	9	9	2	162	7	7.372	1
Fm <sub>3</sub>	Corrosion	7	7	4	196	5	6.302	5
Fm <sub>4</sub>	Erosion	7	6	5	210	4	6.186	7
Fm <sub>5</sub>	Fluid type	5	5	4	100	9	4.767	10
Fm <sub>6</sub>	Input temperature	6	8	5	240	2	6.465	4
Fm <sub>7</sub>	Request temperature	4	9	6	216	3	6.209	6
Fm <sub>8</sub>	Pressure	5	6	8	240	2	6.047	8
Fm <sub>9</sub>	Material	4	4	7	112	8	4.698	11
Fm <sub>10</sub>	Flow array	6	6	5	180	6	5.767	9
Fm <sub>11</sub>	Location	4	3	8	96	10	4.581	12
Fm <sub>12</sub>	Cost	7	7	5	245	1	6.535	3
weight		0.419	0.349	0.232				

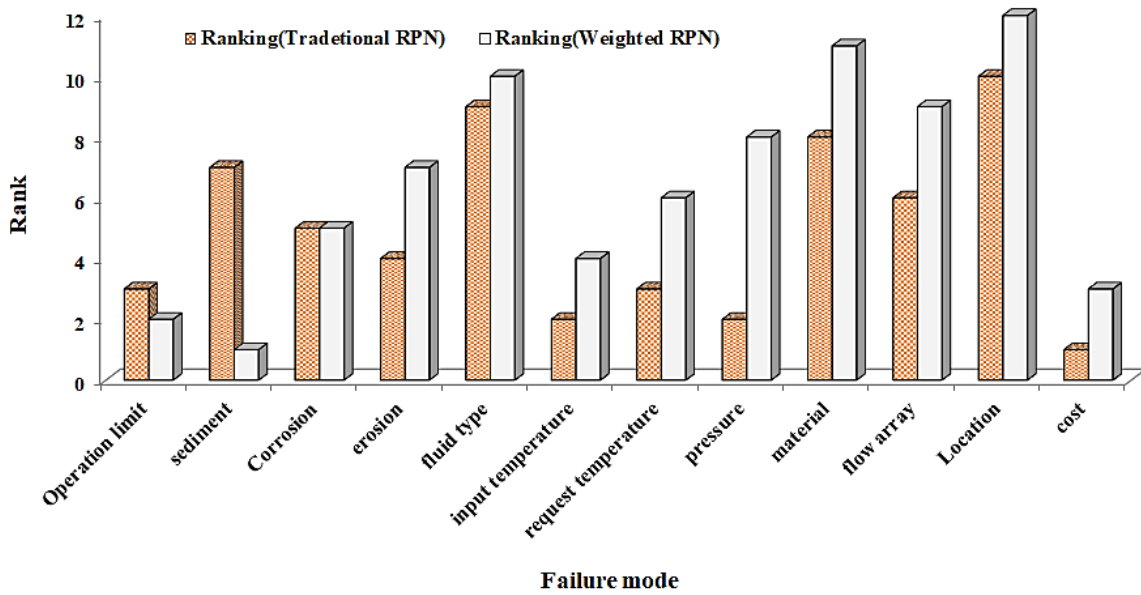


Figure 4: Comparison of traditional and weighted RPNs

6. Sensitivity analysis

According to the data presented in Table 6, the sensitivity of triple factors is investigated by varying their weights. For instance, Case 0 represents the attained weight values of the triple factors in the DVSM weighting procedure, while the others depict distinct weights for feasible scenarios. The results of the positioning of failure modes for various cases are outlined in Table 7 and Figure 5.

In Case 1, there is a 0.1 increase in the weight of the S factor and a corresponding 0.1 reduction in the weights of the O and D factors. Case 2 involves 0.1 increments for the O factor weight and 0.1 decreases in the weights of the S and D factors. Lastly, Case 3 exhibits a 0.1 increase in the weight of the D factor and a 0.1 decrease in the weights of the S and O factors.

Analyzing Table 7 and Figure 5 reveals that in Case 1, certain failure mode ranks have changed. For example, FM10 shifts its rank from 9 to 7, FM4 descends from 7 to 5, FM6 undergoes a change from 4 to 6, and FM7 exhibits a notable difference in rank from 6 to 9. However, some failure modes maintain their positions, such as FM1, FM2, and FM12, retaining ranks 1, 2, and 3, respectively.

In Case 2, failure modes 12, 5, and 10 experience rank changes, with FM12 shifting from 3 to 5, FM5 moving from 10 to 4, and FM10 descending from 7 to 9. On the other hand, FMs 1, 2, 9, and 10 maintain their positions in 2, 1, 11, and 9, respectively.

In Case 3, where the D factor weight is the highest, FM1 and FM2 change their ranks, breaking the consistency observed in previous cases. Specifically, FM3 transitions from 5 to 8, and FM8 descends from 8 to 3. Additionally, FM9 and FM10 retain their ranks at 11 and 9, respectively.

Table 6: Triple factors weight for considered cases

Triple factors	Case 0	Case 1	Case 2	Case 3
S	0.419	0.519	0.319	0.319
O	0.349	0.249	0.449	0.249
D	0.233	0.133	0.133	0.333

Table 7: Ranking results of FMs

Failure modes	Case 0	Case 1	Case 2	Case 3
FM1	2	2	2	1
FM2	1	1	1	2
FM3	5	4	6	8
FM4	7	5	7	7
FM5	10	10	4	12
FM6	4	6	3	5
FM7	6	9	4	6
FM8	8	8	8	3
FM9	11	12	11	11
FM10	9	7	9	9
FM11	12	11	12	10
FM12	3	3	5	4



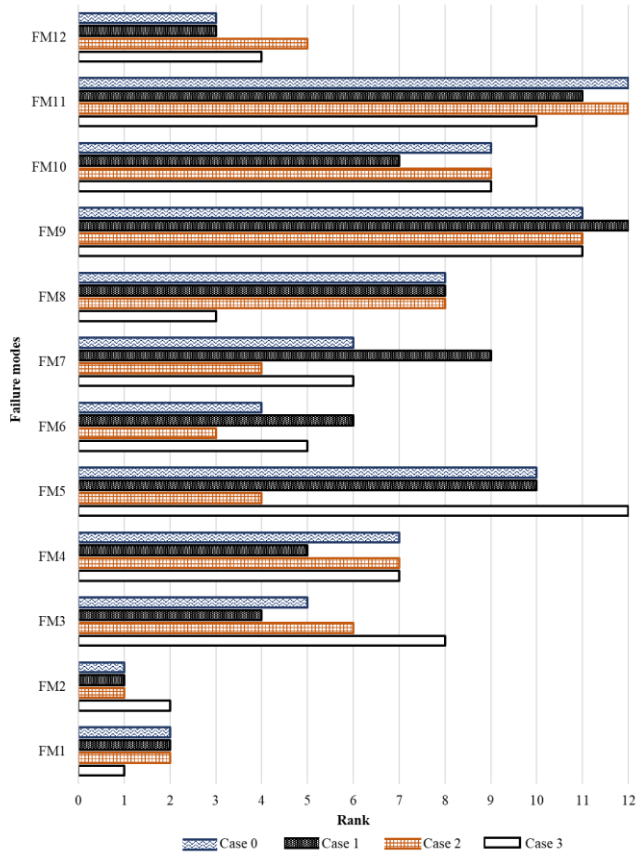


Figure 5: Sensitivity analysis for weighted RPN

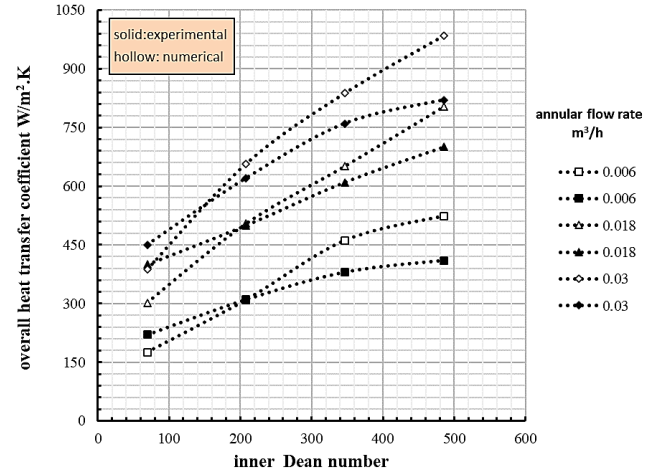


Figure 7: Comparison of experimental and numerical data for overall heat transfer coefficient

where

$$D_e = (Vd/\nu)\sqrt{(d/2R)} \tag{12}$$

$$D_e = (\rho V/\mu)((D_o^2 - D_i^2)/(D_o + D_i))\sqrt{(D_o - D_i)/R} \tag{13}$$

According to the work of [Ogbonnaya and Ajayi \(2017\)](#), fouling rates formula can be recommended as follows:

$$R_f = A/q \tag{14}$$

where  $A = T_{st} - T_{so}$ , such that  $T_{st}$  and  $T_{so}$  are the surface temperature at time t and zero, respectively, and  $q$  is the heat transfer rate. Figure 8 displays the related graph.

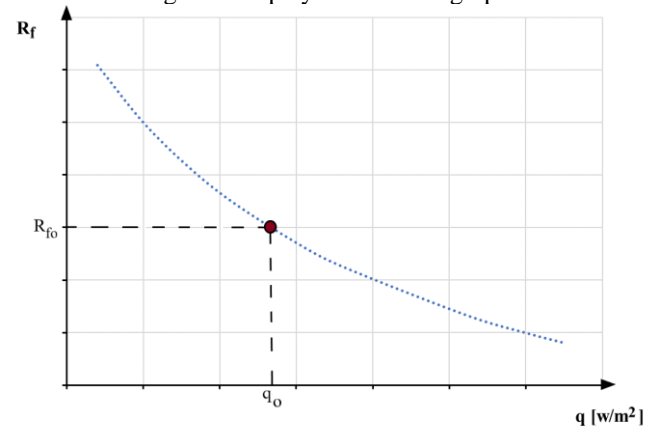


Figure 8: Fouling rate versus heat transfer rate (A was assumed 20 K)

By considering the amount of sediment, Equation 14 can be rewritten as follows:

$$q^{new} = A/R'_f \tag{15}$$

That:

$$R'_f = R_f/(1 - w_s) \tag{16}$$

where  $w_s$  is the weight of severity factor for sediment failure mode (Table 6). By changing the values of  $w_s$ , Figure 9 can be presented.

### 7. Energy analysis

Based on Table 5, this section investigates the effect of the most important parameter on the heat transfer rate. Considering [Pashaee et al. \(2011\)](#) represented data, Figure 6 can be displayed. The Annulus Dean-number for this figure is regarded as 11.93. It should be noted that Figure 7 also shows the validation diagram of the numerical work on the converter. This work is compared with the experimental work of Mr. [Prabhanjan et al. \(2002\)](#). The error value in this graph is approximately 9.3 percent, which is an acceptable error.

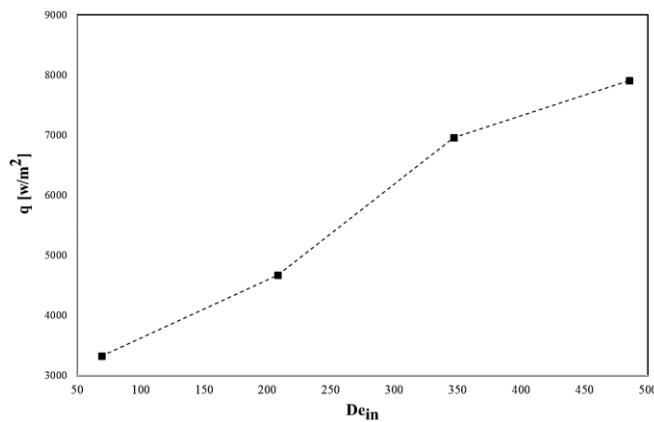


Figure 6: Heat transfer rate for various inner Dean numbers at  $De_{an}=11.93$  ([Pashaee et al., 2011](#))

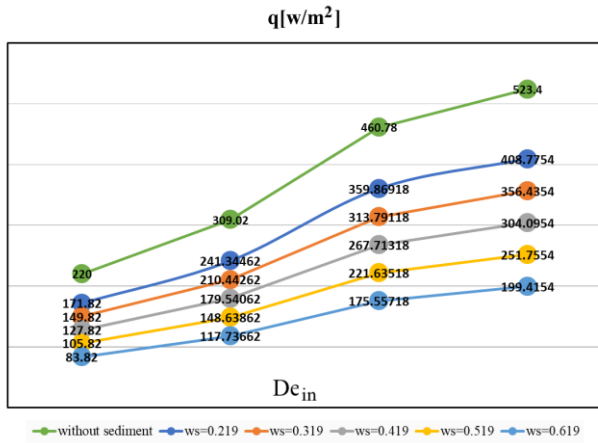


Figure 9: The amount of heat transfer rate versus different fouling rates by applying different  $w_s$

Figure 9 demonstrates that a reduction of almost 65% in fouling rate increases the amount of heat transfer by 105%. This massive increment can decrease energy consumption and improve system efficiency. Considering efficiency as follows:

$$\eta = q_f / q_{without\ sediment} \times 100 \quad (17)$$

Figure 10 displays the amount of system efficiency for various modes. It is evident that the more sediment, the less system efficiency. When  $w_{s1} = 0.219$ , the efficiency is  $\eta_1 = 78.1\%$  while if  $w_{s5} = 0.619$ , then the efficiency has a value of  $\eta_5 = 38.1\%$ .

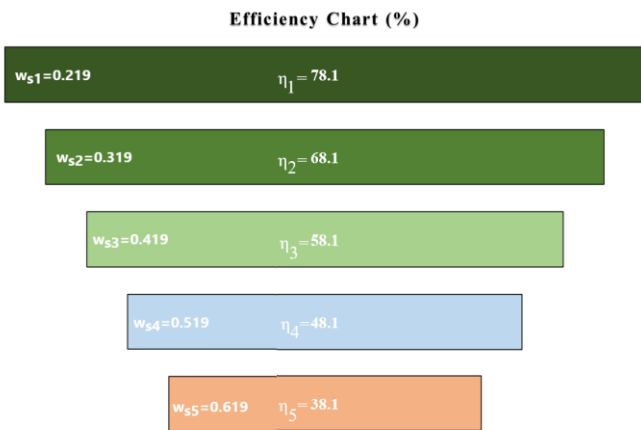


Figure 10: Comparison of efficiencies for different modes

The presented analysis demonstrates that accounting for the impact of failure factors can deviate numerical results from the ideal state, bringing them closer to real-world outcomes. This analysis holds significant importance, especially in highly advanced industrial designs, such as those in the aerospace and medical industries. It enables designers to ground their final analyses on more realistic data.

Another analysis that warrants mention is the impact of sedimentation on energy and economic assessments. Figure 11 illustrates the energy loss over time, specifically for  $W_s=0.619$ . Through effective sedimentation management, Figure 12 depicts potential energy and cost savings.

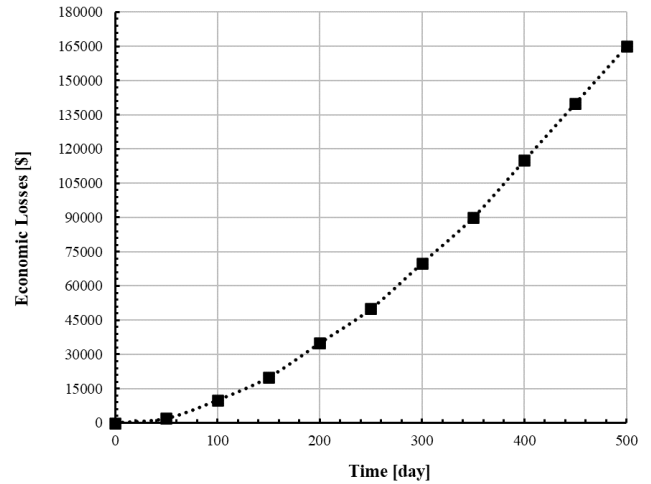


Figure 11: Losses through time for heat exchanger

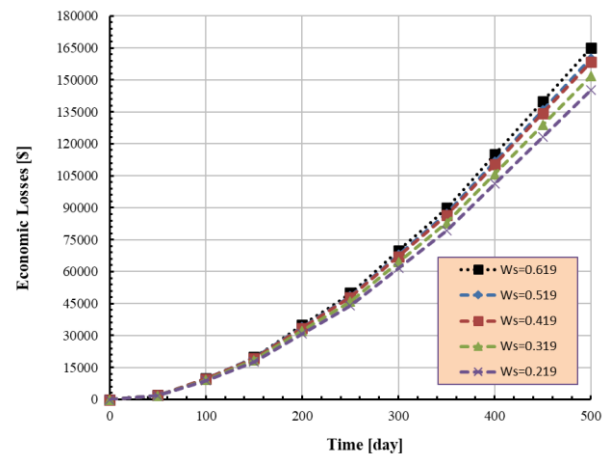


Figure 12: Losses through time for various  $W_s$

Figure 12 states that the amount of economic savings and therefore energy savings from  $W_s=0.619$  to  $W_s=0.219$  is about 12%, which is a significant amount.

### 8. CONCLUSION

Risk evaluation is a crucial aspect of system design, gaining increasing prominence in the design process. The Failure Mode and Effect Analysis (FMEA) method, designed to furnish information for risk management, finds widespread application across various domains. In FMEA, Failure Modes (FMs) are determined and evaluated through risk factors categorized as Severity (S), Occurrence (O), and Detection (D). In a typical FMEA, the risk rank of each failure mode is computed by multiplying the raw values of the risk factors.

This study introduces the Deviation Value Step-Wise Method (DVSM) to derive scores for Severity, Occurrence, and Detection (SOD) factors, thereby prioritizing failure modes. Following the identification of Failure Modes using the FMEA technique, DVSM assigns weights to the SOD factors, addressing a shortcoming of the conventional Risk Priority Number (RPN) value, which lacks the consideration of different weights for determinant factors. The outcomes demonstrate the effectiveness of this approach in achieving comprehensive prioritization of failure modes.

The proposed methodology empowers decision-makers to identify critical failure modes based on nuanced differentiation, enabling the formulation of corrective/preventive actions within the constraints of

available resources. Application of this approach to analyze failure modes in a dual-tube heat exchanger, in comparison to traditional FMEA, reveals more pragmatic results. For instance, failure modes FM6 and FM8, jointly ranked second based on conventional RPN scores, are repositioned to fourth and eighth positions, respectively, with the proposed approach. Furthermore, sensitivity and energy analyses, involving varying weights of SOD in four scenarios, underscore the impact on the repositioning of failure modes.

Examining the most critical failure mode, sediment, and its effect on the system's heat transfer rate and energy efficiency, the results highlight a 65% reduction in fouling rate leading to a 105% increase in energy efficiency. Economic and energy-saving analysis indicates substantial savings, ranging from  $W_s=0.619$  to  $W_s=0.219$ , amounting to about 12%. This signifies a significant contribution to the overall understanding and optimization of the system under consideration.

## 9. ACKNOWLEDGEMENT

We are grateful to the management of Science based TMco for their cooperation in carrying out this project.

## NOMENCLATURE

a	alternative
c	criteria
De	Dean number
Fm	Failure mode
v	velocity
w	weight
z	Request function
<b>Greek letters</b>	
$\mu$	viscosity
$\eta$	efficiency
<b>Subscripts</b>	
i	inner
o	outer

## REFERENCES

- Abu-Hamdeh, N. & Salilih, E., (2020), Numerical modeling of a parallel flow heat exchanger with the two-phase heat transfer process, *International Communications in Heat and Mass Transfer*, <https://doi.org/10.1016/j.icheatmasstransfer.2020.105005>
- Almerbati, A., (2021), Hexagonal and mixed arrays of flow channel design in the counterflow heat exchanger, *International Communications in Heat and Mass Transfer*, *124*, 105268. <https://doi.org/10.1016/j.icheatmasstransfer.2021.105268>
- Avikal, S., Singh, A., Kumar, K. & Badhotiya, G. (2021), A fuzzy-AHP and TOPSIS based approach for selection of metal matrix composite used in the design and structural applications, *Materials Today: Proceedings*. <https://doi.org/10.1016/j.matpr.2021.02.161>
- Baghbani, M., Iranzadeh, S. & khajeh, M., (2019), Investigating the relationship between RPN parameters in fuzzy PFMEA and OEE in a sugar factory, *Journal of Loss Prevention in the Process Industries*, Volume 60, Pages 221-232. <https://doi.org/10.1016/j.jlp.2019.05.003>
- Bahrami, Y., Hassani, H. & Maghsoudi, A., (2019), BWM-ARAS: A new hybrid MCDM method for Cu prospectivity mapping in the Abhar area, NW Iran, *Spatial Statistics*, *33*, 100382. <https://doi.org/10.1016/j.spasta.2019.100382>
- Balali, A., Valipour, A., Edwards, R. & Moehler, R., (2021), Ranking effective risks on human resources threats in natural gas supply projects using ANP-COPRAS method: Case study of Shiraz, *Reliability Engineering & System Safety*, *208*, 107442. <https://doi.org/10.1016/j.ress.2021.107442>
- Baležentis, A. Baležentis, T. & Brauers, W.K. (2012), Personnel selection based on computing with words and fuzzy MULTIMOORA, *Expert Systems with Applications*, *39* (9), 7961-7967. <https://doi.org/10.1016/j.eswa.2012.01.100>
- Balki, M., Erdoğan, S., Aydın, S. & Sayin, C., (2020), The optimization of engine operating parameters via SWARA and ARAS hybrid method in a small SI engine using alternative fuels, *Journal of Cleaner Production*, *258*, 120685. <https://doi.org/10.1016/j.jclepro.2020.120685>
- Benmoussa, K., Laaziri, M., Khouliji, S., Kerkeb, M. & Yamami, A., (2019), AHP-based Approach for Evaluating Ergonomic Criteria, *Procedia Manufacturing*, *32*, Pages 856-863. <https://doi.org/10.1016/j.promfg.2019.02.294>
- Chen, J., Chen, S., Fu, R., Wang, C., Li, D., Jiang, H., Zhao, J., Wang, L., Peng, Y. & Mei, Y., (2021), Simulation of water hyacinth growth area based on multi-source geographic information data: An integrated method of WOE and AHP, *Ecological Indicators*, *125*, 107574. <https://doi.org/10.1016/j.ecolind.2021.107574>
- Chin, K. S., Chan, A., & Yang, J. B. (2008). Development of a fuzzy FMEA based product design system. *International Journal of Advanced Manufacturing Technology*, *36*, 633–649. <https://doi.org/10.1007/s00170-006-0898-3>
- Chodha, V., Dubey, R., Kumar, R., Singh, S. & Kaur, S., (2021), Selection of industrial arc welding robot with TOPSIS and Entropy MCDM techniques, *Materials Today: Proceedings*, *50* (9). <https://doi.org/10.1016/j.matpr.2021.04.487>
- Dorosti, S., Fathi, M., Ghouschi, S., Khakifirooz, M. & Khazaeili, M., (2020), Patient waiting time management through fuzzy-based failure mode and effect analysis, *Journal of Intelligent & Fuzzy Systems*, *38*, no. 2, pp. 2069-2080. <https://doi.org/10.3233/JIFS-190777>
- Eduardo, C., (2010), Heat Transfer in Process Engineering, McGraw-Hill Education. <https://www.accessengineeringlibrary.com/content/book/9780071624084>
- Ghouschi, S., Yousefi, S. & Khazaeili, M., (2019), An extended FMEA approach based on the Z-MOORA and fuzzy BWM for prioritization of failures, *Applied Soft Computing*, *81*, 105505. <https://doi.org/10.1016/j.asoc.2019.105505>
- Ghouschi, S. & Khazaeili, M., (2019), G-Numbers: Importance-Necessity Concept in Uncertain Environment, *International Journal of Management and Fuzzy Systems*; *5*(1): 27-32. <https://doi.org/10.11648/j.ijmfs.20190501.15>
- Ghouschi, S.J.; Dorosti, S.; Khazaeili, M. & Mardani, A. (2021), Extended approach by using best-worst method on the basis of importance—Necessity concept and its application. *Appl. Intell.* 1–15. <https://doi.org/10.1007/s10489-021-02316-3>
- Ghouschi, S., Khazaeili, M., Amini, A. & Osgooei, E., (2019), Multi-criteria sustainable supplier selection using piecewise linear value function and fuzzy best-worst method, *Journal of Intelligent & Fuzzy Systems*, *37*, no. 2, pp. 2309-2325, <https://doi.org/10.3233/jifs-182609>
- Hoisaik, J., Manger, R., Dragojević, I., (2021), Benchmarking failure mode and effects analysis of electronic brachytherapy with data from incident learning systems, *Brachytherapy*, <https://doi.org/10.1016/j.brachy.2020.11.014>
- Hu, J., Xu, B., Chen, Z., Zhang, H., Cao, J., Wang, Q., (2021), Hazard and risk assessment for hydraulic fracturing induced seismicity based on the Entropy-Fuzzy-AHP method in Southern Sichuan Basin, China, *Journal of Natural Gas Science and Engineering*, *90*, 103908. <https://doi.org/10.1016/j.jngse.2021.103908>
- Jafarzadeh Ghouschi, S.; Khazaeili, M.; Sabri-Laghaie, K. (2019), An extended Multi-Criteria Green Supplier Selection based on Z-Numbers for Fuzzy Multi-Objective Linear Programming Problem. *Int. J. Ind. Eng. Manag. Sci.*, *6*, 74–96. [https://www.ijiems.com/article\\_90013.html](https://www.ijiems.com/article_90013.html)
- Khalilzadeh, M., Shakeri, H., Zohrehvandi, S., (2021), Risk identification and assessment with the fuzzy DEMATEL-ANP method in oil and gas projects under uncertainty, *Procedia Computer Science*, *181*, Pages 277-284. <https://doi.org/10.1016/j.procs.2021.01.147>

23. Kumar, N.T.R., Bhrumara, P., Kirubeil, A., Syam Sundar, L., Singh, M., Sousa, A.C.M., (2018), Effect of twisted tape inserts on heat transfer, the friction factor of Fe<sub>3</sub>O<sub>4</sub> nanofluids flow in a double pipe U-bend heat exchanger, *International Communications in Heat and Mass Transfer*, 95, Pages 53-62. <https://doi.org/10.1016/j.icheatmasstransfer.2018.03.020>
24. Lahri, V., Shaw, K. & Ishizaka, A., (2021), Sustainable supply chain network design problem: Using the integrated BWM, TOPSIS, possibilistic programming, and  $\epsilon$ -constrained methods, *Expert Systems with Applications*, 168, 114373. <https://doi.org/10.1016/j.eswa.2020.114373>
25. Li, X., Wang, L., Feng, R., Wang, Z., Liu, Sh. & Zhu, D., (2021), Study on shell side heat transport enhancement of double tube heat exchangers by twisted oval tubes, *International Communications in Heat and Mass Transfer*, 124, 105273. <https://doi.org/10.1016/j.icheatmasstransfer.2021.105273>
26. Lin, S., Shen, S., Zhang, N. & Zhou, A., (2021), Comprehensive environmental impact evaluation for concrete mixing station (CMS) based on improved TOPSIS method, *Sustainable Cities and Society*, 69, 102838. <https://doi.org/10.1016/j.scs.2021.102838>
27. Liu, Z., Li, Y. & Zhou, K., (2016), Thermal analysis of double-pipe heat exchanger in the thermodynamic vent system, *Energy Conversion and Management*, 126, Pages 837-849. <http://dx.doi.org/10.1016/j.enconman.2016.08.065>
28. Long, D. & Hillman, M., (2014), Chapter 17 - Introduction: Medical Engineering Design, Regulations, and Risk Management, *Clinical Engineering, A Handbook for Clinical and Biomedical Engineers*, Pages 257-274. <https://ieeexplore.ieee.org/document/7059338>
29. Luo, C., Ju, Y., Gonzalez, E., Dong, P. & Wang, A., (2020), The waste-to-energy incineration plant site selection based on hesitant fuzzy linguistic Best-Worst method ANP and double parameters TOPSIS approach: A case study in China, *Energy*, Volume 211, 118564. <https://doi.org/10.1016/j.energy.2020.118564>
30. Ma, Y., Wei, J., Li, C., Liang, C. & Liu, G., (2020), Fuzzy comprehensive performance evaluation method of rolling linear guide based on improved analytic hierarchy process, *Journal of Mechanical Science and Technology*, 34, pages 2923–2932. <https://doi.org/10.1007/s12206-020-0624-3>
31. Maakoul, A., Feddi, K., Saadeddine, S., Abdellah, A. & Metoui, M., (2020), Performance enhancement of finned annulus using surface interruptions in double-pipe heat exchangers, *Energy Conversion and Management*, 210, 112710. <https://doi.org/10.1016/j.enconman.2020.112710>
32. Maakoul, A., Laknizi, A., Saadeddine, S., Abdellah, A., Meziane, M. & Metoui, M., (2017), Numerical design and investigation of heat transfer enhancement and performance for an annulus with continuous helical baffles in a double-pipe heat exchanger, *Energy Conversion and Management*, 133, Pages 76-86. <https://doi.org/10.1016/j.enconman.2016.12.002>
33. Maddah, H., Aghayari, R., Mirzaee, M., Ahmadi, M., Sadeghzadeh, M., Chamkhade, A.J., (2018), Factorial experimental design for the thermal performance of a double pipe heat exchanger using Al<sub>2</sub>O<sub>3</sub>-TiO<sub>2</sub> hybrid nanofluid, *International Communications in Heat and Mass Transfer*, 97, Pages 92-102. <https://doi.org/10.1016/j.icheatmasstransfer.2018.07.002>
34. Mehrabi, M., Pesteei, S.M. & Pashae Golmarz T., (2011), Modeling of heat transfer and fluid flow characteristics of helicoidal double-pipe heat exchangers using Adaptive Neuro-Fuzzy Inference System (ANFIS), *International Communications in Heat and Mass Transfer*, 38, Issue 4, Pages 525-532. <https://doi.org/10.1016/j.icheatmasstransfer.2010.12.025>
35. Mehrabi, M., Golmarz, T.P., Sharifpur, M., Meyer, J.P., (2013), Application of genetic algorithm-polynomial neural network for modeling heat transfer and fluid flow characteristics of a double-pipe heat exchanger, *Proceedings of the ASME Heat Transfer Summer Conference*, Minneapolis, MN, USA. <https://doi.org/10.1115/ht2013-17194>
36. Miciuła, I. & Grunt, J., (2019), Using the AHP method to select an energy supplier for a household in Poland, *Procedia Computer Science*, 159, Pages 2324-2334. <https://doi.org/10.1016/j.procs.2019.09.407>
37. Ogbonnaya, S. & Ajayi, O., (2017), Fouling phenomenon and its effect on heat exchanger: A review, *Frontiers in Heat and Mass Transfer (FHMT)*, 9, 31. <https://doi.org/10.5098/hmt.9.31>
38. Okabe, T. & Otsuka, Y., (2021), Proposal of a Validation Method of Failure Mode Analyses based on the Stress-Strength Model with a Support Vector Machine, *Reliability Engineering & System Safety*, 205, 107247. <https://doi.org/10.1016/j.res.2020.107247>
39. Ouyang, L., Zhu, Y., Zheng, W. & Yan, L., (2021), An information fusion FMEA method to assess the risk of healthcare waste, *Journal of Management Science and Engineering*, 6, Issue 1, Pages 111-124. <https://doi.org/10.1016/j.jmse.2021.01.001>
40. Pashae Golmarz, T. & Pesteei, S.M., (2012), Investigation of Dean number and curvature ratio in a double-pipe helical heat exchanger, *International Conference on Mechanical Engineering-ISME School of Mechanical Eng.*, Shiraz University, Shiraz, Iran. <https://civilica.com/doc/151470/>
41. Pashae Golmarz, T., Rezazadeh, S. & Bagherzadeh, N., (2018), Numerical study of curved-shape channel effect on performance and distribution of species in a proton-exchange membrane fuel cell: Novel structure. *J. Renew. Energy Environ.*, 5, 10–21. <https://doi.org/10.30501/jree.2018.88506>
42. Pashae Golmarz, T., Rezazadeh, S., Yaldagard, M. & Bagherzadeh, N. (2021), The Effect of Proton-Exchange Membrane Fuel Cell Configuration Changing from Straight to Cylindrical State on Performance and Mass Transport: Numerical Procedure, *J. Renew. Energy Environ.*, 8, 39–53. <https://doi.org/10.30501/jree.2020.253825.1152>
43. Prabhanjan, D.G., Raghavan, G.S.V. & Rennie, T.J. (2002), Comparison of heat transfer rates between a straight tube heat exchanger and a helically coiled heat exchanger, *International Communications in Heat and Mass Transfer*, 29 (2), 185–191. [https://doi.org/10.1016/S0735-1933\(02\)00309](https://doi.org/10.1016/S0735-1933(02)00309)
44. Qi, C., Luo, t., Liu, m., Fan, F. & Yan, Y., (2019), Experimental study on the flow and heat transfer characteristics of nanofluids in double-tube heat exchangers based on thermal efficiency assessment, *Energy Conversion, and Management*, 197, 111877. <https://doi.org/10.1016/j.enconman.2019.111877>
45. Rezaei, J., (2015), Best-worst multi-criteria decision-making method, *Omega*, 53, 49–57. <https://doi.org/10.1016/j.omega.2014.11.009>
46. Sari, F., (2021), Forest fire susceptibility mapping via multi-criteria decision analysis techniques for Mugla, Turkey: A comparative analysis of VIKOR and TOPSIS, *Forest Ecology and Management*, 480, 118644. <https://doi.org/10.1016/j.foreco.2020.118644>
47. Sedghiyan, D., Ashouri, A., Maftouni, N., Xiong, Q., Rezaee, E. & Sadeghi, S., (2021), Prioritization of renewable energy resources in five climate zones in Iran using AHP, hybrid AHP-TOPSIS, and AHP-SAW methods, *Sustainable Energy Technologies, and Assessments*, 44, 101045. <https://doi.org/10.1016/j.seta.2021.101045>
48. Schmid, G., Huang, Z., Yang, T. & Chen, S., (2017), Numerical analysis of a vertical double-pipe single-flow heat exchanger applied in an active cooling system for high-power LED street lights, *Applied Energy*, 195, Pages 426-438. <https://doi.org/10.1016/j.apenergy.2017.03.054>
49. Subriadi, A. & Najwa, N., (2020), The consistency analysis of failure mode and effect analysis (FMEA) in information technology risk assessment, *Heliyon*, 6, Issue 1, 03161. <https://doi.org/10.1016/j.heliyon.2020.e03161>
50. Targui, N. & Kahalerras, H., (2008), Analysis of fluid flow and heat transfer in a double pipe heat exchanger with porous structures, *Energy Conversion and Management*, 49, Issue 11, Pages 3217-3229. <https://doi.org/10.1016/j.enconman.2008.02.010>
51. Torkayesh, A., Zolfani, S., Kahvand, M. & Khazaelpour, P., (2021), Landfill location selection for healthcare waste of urban areas using hybrid BWM-grey MARCOS model based on GIS, *Sustainable Cities, and Society*, 67, 102712. <https://doi.org/10.1016/j.scs.2021.102712>



52. Vasauskas, V., Baskutis, S., (2006), Failures and fouling analysis in heat exchangers, *Mechanika.. NR.5* (61).  
<https://mechanika.ktu.lt/index.php/Mech/article/view/14758>
53. Wang, Y., Sun, B., Zhang, X., Wang, Q., (2020), BWM, and MULTIMOORA-based multi granulation sequential three-way decision model for multi-attribute group decision-making problem, *Approximate Reasoning*, 125, Pages 169-186.  
<https://doi.org/10.1016/j.ijar.2020.07.003>
54. Wenju, H., Mengjie, S., Yiqiang, J., Yang, Y. & Yan, G., (2019), A modeling study on the heat storage and release characteristics of a phase change material based double-spiral coiled heat exchanger in an air source heat pump for defrosting, *Applied Energy*, 236, Pages 877-892. <https://doi.org/10.1016/j.apenergy.2018.12.057>
55. Xing, H., Jiang, T. & Hao, P., (2021), An efficient dominant failure modes search strategy and an extended sequential compounding method of system reliability analysis and optimization, *Computer Methods in Applied Mechanics and Engineering*, Volume 375, 113637.  
<https://doi.org/10.1016/j.cma.2020.113637>
56. Yücenur, G. & Ipekçi, A., (2021), SWARA/WASPAS methods for a marine current energy plant location selection problem, *Renewable Energy*, 163, Pages 1287-1298  
<https://doi.org/10.1016/j.renene.2020.08.131>
57. Yildiz, C., Biçer, Y. & Pehlivan, D., (1996), Influence of fluid rotation on the heat transfer and pressure drop in double-pipe heat exchangers, *Applied Energy*, 54, Issue 1, Pages 49-56.  
[https://doi.org/10.1016/0306-2619\(95\)00070-4](https://doi.org/10.1016/0306-2619(95)00070-4)
58. Zanchini, E. & Jahanbin, A., (2017), Correlations to determine the mean fluid temperature of double U-tube borehole heat exchangers with a typical geometry, *Applied Energy*, 206, Pages 1406-1415.  
<https://doi.org/10.1016/j.apenergy.2017.09.120>
59. Zanchini, E. & Jahanbin, A., (2018), Simple equations to evaluate the mean fluid temperature of double-U-tube borehole heat exchangers, *Applied Energy*, 231, Pages 320-330.  
<https://doi.org/10.1016/j.apenergy.2018.09.094>
60. Zarrella, A., Capozza, A. & Carli, M., (2013), Analysis of short helical and double U-tube borehole heat exchangers: A simulation-based comparison, *Applied Energy*, 112, Pages 358-370.  
<https://doi.org/10.1016/j.apenergy.2013.06.032>